Dlx2 homeobox gene transcriptional regulation of Trkb neurotrophin receptor expression during mouse retinal development

Jimmy de Melo[1], Qing-Ping Zhou[2], Qi Zhang[1], Shunzhen Zhang[2,3], Mario Fonseca[1,2], Jeffrey T. Wigle[4,5] and David D. Eisenstat[1–4,6,*]

[1]Department of Human Anatomy and Cell Science, [2]Manitoba Institute of Cell Biology, [3]Department of Pediatrics and Child Health, [4]Department of Biochemistry and Medical Genetics, [5]St Boniface General Hospital Research Centre and [6]Department of Ophthalmology, University of Manitoba, Winnipeg, Manitoba, Canada R3E 0V9

ABSTRACT

***Dlx* homeobox genes are first expressed in embryonic retina at E11.5. The *Dlx1/Dlx2* null retina has a reduced ganglion cell layer (GCL), with loss of late-born differentiated retinal ganglion cells (RGCs) due to increased apoptosis. TrkB signaling is proposed to regulate the dynamics of RGC apoptosis throughout development. DLX2 expression markedly precedes the onset of TrkB expression in the GCL; TrkB co-expression with *Dlx2* and RGC markers is well-established by E13.5. In the *Dlx1/Dlx2* null retina, *TrkB* expression is significantly reduced by E16.5. We demonstrated that DLX2 binds to a specific region of the TrkB promoter in retinal neuroepithelium during embryogenesis. *In vitro* confirmation and the functional consequences of DLX2 binding to this TrkB regulatory region support TrkB as a *Dlx2* transcriptional target. Furthermore, ectopic *Dlx2* expression in retinal explants activates TrkB expression and *Dlx2* knockdown in primary retinal cultures results in reduced TrkB expression. RGC differentiation and survival require the coordinated expression of transcription factors. This study establishes a direct transcriptional relationship between a homeodomain protein involved in RGC differentiation and a neurotrophin receptor implicated in RGC survival. Signaling mediated by TrkB may contribute to survival of late-born RGCs whose terminal differentiation is regulated by *Dlx* gene function.**

INTRODUCTION

During vertebrate retinogenesis several distinct cell types are generated from retinal progenitors (1). In the mouse, retinal ganglion cells (RGCs) are generated first followed by cones, horizontal cells, amacrine cells, rods, bipolar cells and Müller glia (2–4). In the murine retina, RGCs are born between embryonic day (E) 10 and postnatal day (P) 2 with a maximal birth rate at E15. Cell death occurs during RGC genesis in two distinct phases (5). The first phase occurs at E15.5 and corresponds with the peak of RGC neurogenesis (6). The second occurs after birth, peaking at P2 and correlates with the elaboration of RGC projections to the superior colliculus (SC) (7).

The vertebrate *Distal-less* (*Dlx*) homeobox gene family consists of six murine members (8) organized into three bigenic gene clusters (9–11). Four *Dlx* family members have been implicated in neurogenesis in the mouse: *Dlx1*, *Dlx2*, *Dlx5* and *Dlx6* (12–14) with *Dlx1* and *Dlx2* further implicated in retinogenesis (15–17). Previous work established that *Dlx1* and *Dlx2* are both expressed in the retinal neuroepithelium by E12.5 (15). Expression of *Dlx1* becomes largely restricted to the ganglion cell layer (GCL); perinatally, its expression is down-regulated. *Dlx2* is expressed throughout the lifetime of the mouse with expression becoming restricted to RGCs, amacrine and horizontal cells (16). Characterization of the *Dlx1/Dlx2* null mouse demonstrated loss of approximately one-third of RGCs at E18.5 (17). *Dlx1/Dlx2* mutant retinas contain disproportionately higher numbers of RGCs born prior to E13.5 and a decreased population of later born RGCs, with loss of RGCs due to increased apoptosis between E13.5 and E18.5 (17). RGC numbers in the adult *Dlx1/Dlx2* mutant retina cannot be determined as mutants die perinatally. The molecular mechanisms underlying RGC apoptosis in the *Dlx1/Dlx2* double knockout retina have not been established.

TrkB, a member of the neurotrophin receptor family encoded by the *NTRK2* gene, demonstrates specific binding affinity for brain derived neurotrophic factor (BDNF) and neurotrophin NT4/5 (18–20). Target-derived BDNF signaling via TrkB modulates cell death during

---

*To whom correspondence should be addressed. Tel: 204 787 1169; Fax: 204 787 2190; Email: eisensta@cc.umanitoba.ca

RGC neurogenesis (21). Null mutation of the catalytic domain of the $TrkB_{FL}$ receptor results in a dose-dependent increase in the peak RGC death rate, although final RGC numbers remain normal (22).

To investigate the role of *Dlx* genes in the processes of RGC differentiation and survival, we have tested the hypothesis that DLX2 regulates TrkB expression during retinal development. We show that DLX2 expression precedes TrkB in the embryonic GCL by 1–2 days with DLX2 expressing retinal neuroepithelial cells co-expressing TrkB upon migration to the inner retina. As well, DLX2 directly binds to a specific TrkB proximal promoter region *in vivo*, and functions as a transcriptional activator of TrkB expression *in vitro*. We also demonstrate that loss or gain of *Dlx2* function results in a corresponding decrease or increase of TrkB expression within the developing retina.

MATERIALS AND METHODS

Animal and tissue preparation

Wild-type tissues were obtained from the CD-1 (ICR) BR Swiss strain of albino mice (Charles River Laboratories, Worcester, MA, USA). *Dlx1/Dlx2* knockout mice were generated as previously described (13,23). Embryonic age was determined by the day of appearance of the vaginal plug (E0.5) and confirmed by morphological criteria. For immunostaining studies, E16.5 and E18.5 eyes were dissected from embryos while E13.5 eyes were left *in situ*. Tissues were processed as previously described (16). All animal protocols were conducted in accordance with guidelines set by the Canadian Council on Animal Care and the University of Manitoba animal care committee. *Dlx1/Dlx2* null mice were genotyped as described (24). For comparative studies, all *Dlx1/Dlx2* mutants were paired with wild-type littermate controls.

Immunohistochemistry and immunofluorescence

Immunohistochemistry and immunofluorescence staining on cryosections were performed as described (16). Primary antibodies used were: rabbit anti-BRN3b (1 : 200, Babco, Richmond, CA, USA), goat anti-BRN3b (1 : 200, Santa Cruz, Santa Cruz, CA, USA), mouse anti-Chat (1 : 100, Chemicon, Temacula, CA, USA), rabbit anti-CHX10 (1 : 700, courtesy Dr T. Jessell, Columbia University), rabbit anti-DLX2 (1 : 250), mouse anti-ISLET-1 (1 : 600, Developmental Studies Hybridoma Bank, University of Iowa, IA, USA), mouse anti-NF165 (1 : 50, Developmental Studies Hybridoma Bank, University of Iowa, IA, USA), rabbit anti-PROX1 (1 : 500, courtesy Dr M. Nakafuku, University of Tokyo), mouse anti-Rho4D2 (1 : 80, courtesy Dr R. Molday, University of British Columbia), mouse anti-Syntaxin (1 : 6000, Sigma, St Louis, MO, USA), rabbit anti-TrkB (1 : 200, Santa Cruz). Peanut Agglutinin (PNA) (1 : 2000, Vector Laboratories, Burlingame, CA, USA) staining was also used for detection of cone photoreceptors. Secondary antibodies and fluorescent tertiary molecules used were FITC-conjugated goat anti-rabbit (1 : 100, Sigma), Texas red-conjugated donkey anti-rabbit (1 : 200, Jackson Immunoresearch, West Grove, PA, USA), Texas red-conjugated donkey anti-mouse (1 : 200, Jackson Immuno-research), Texas red-conjugated donkey anti-goat (1 : 200, Jackson Immunoresearch). Peanut agglutinin was visualized using streptavidin-conjugated Texas Red (1 : 200, Vector Laboratories). Negative controls omitted the primary antibody.

Chromatin immunoprecipitation (ChIP) assays

ChIP assays were performed as described previously using E16.5 retinal tissues (25). Oligonucleotide primers were designed according to distinct regions of the TrkB gene sequence (Ensemble Gene ID: ENSMUSG0000055254). Region 1 (R1-pro) was located within the 5′ proximal promoter 842 bp upstream of the transcription start site. For R1-pro, the sense primer was 5′-CAGAGAGCATC TCTGAGAG-3′ and the anti-sense primer was 5′-GCA CTGCCTTTCTGA-CTGG-3′. Six other regions of the proximal TrkB promoter were also assessed (refer to Supplementary Figure 4 and legend for oligonucleotide primer sequences). Polymerase chain reaction (PCR) was performed on genomic DNA derived from E16.5 mouse embryos as a positive control. PCR products were separated by gel electrophoresis, purified and then ligated into the pCR2.1 TOPO vector using a TOPO TA cloning kit (Invitrogen, Burlington, ON, USA). Recombinant plasmid DNA was extracted using a MiniPrep Kit (Qiagen Inc., Mississauga, ON, USA) and M13 reverse universal primer was used for confirmation of sequence.

Nuclear extracts and gel shift assays

Liver or retina tissues were obtained from wild-type CD1 mice at E13.5 and triturated in 1× PBS to obtain single cell suspensions. Following centrifugation at 200 r.p.m., 1 ml of Buffer A (20 mM HEPES/KOH pH 7.5, 10 mM KCl, 1.5 mM MgCl₂, 1 mM EDTA, 1 mM EGTA, 1 mM DTT, 250 mM sucrose) was added to the pellet, placed on ice (15 min) and the suspension was then passed 40 times through a 26G 0.5″ needle and spun at 4500 r.p.m. (10 min.). The pellet was then washed with Buffer A and 10 μl of 10% NP-40 was added, rotated at 4°C (10 min.), spun at 13 000 r.p.m. (15 min.) and then 200 μl of Nuclear Extraction Buffer (20 mM HEPES/KOH pH 7.9, 420 mM NaCl, 1.5 mM MgCl₂, 0.2 mM EDTA, 0.5 mM DTT, 25% glycerol) was added to the pellet, rotated at 4°C (30 min.), spun at 13 000 r.p.m. (15 min.) and the resultant supernatant was used as nuclear extract.

Electrophoretic mobility gel shift assays (EMSA) were performed as reported previously (25). The TrkB promoter region was digested with EcoRI, then the 5′ overhang was filled in with the large fragment of DNA polymerase I (Klenow) in the presence of radiolabeled (α^{32}P) dATP. Recombinant protein of 100 ng or 1 μg of nuclear extract was used per reaction. For 'cold competition' assays, double-stranded unlabeled fragments were added at 100-fold excess. For 'supershift' assays, specific polyclonal DLX2 antibodies were used; a rabbit polyclonal antibody to mouse immunoglobulin G (Jackson Immunoresearch) was utilized as an antibody control. Sequences of the two putative TAAT/ATTA homeodomain binding motifs from the TrkB promoter region were used to generate

individual synthetic oligonucleotides (25–30 bp, Sigma). Double-stranded oligonucleotides were incubated with the T4 polynucleotide kinase (T4 PNK) and α^{32}P-ATP. Nuclear extracts were incubated with 1× binding buffer, poly(dI-dC), 1 mM PMSF and P^{32}-labeled DNA probes. For 'cold competition' assays, unlabeled double-stranded oligonucleotides were added at 100-fold excess. Reactions were resolved on a 4% non-denaturing polyacrylamide (37.5: 1 acrylamide/bisacrylamide) gel in 0.5× Tris–Borate–EDTA solution. Gels were exposed to film and autoradiography was performed overnight at −70°C. Motif P-TrkB1: sense primer: 5′-CCAGCATTC**ATTAG**ACTCTTCCTGTC-3′, antisense primer: 5′-GACAGGAAGAGTC**TAAT**GAATGCTGG-3′; motif PM-TrkB1 (mutant): sense primer: 5′-CCAGCATTC**AGGAG**ACTCTTCCTGTC-3′, antisense primer: 5′ GACAGGAAGAGTC**TCCT**GAATGCTGG-3′; motif P-TrkB2: sense primer: 5′-GGAGTGGGGCAGT**AATTA**CTCCTCCCTTCC-3′, antisense primer: 5′- GGAAGGGAGGAGT**AATTA**CTGCCCCACTCC-3′; motif PM-TrkB2 (mutant): sense primer: 5′- GGAGTGGGGCAGT**AGTTA**CTCCTCCCTTCC-3′, antisense primer: 5′-GGAAGGGAGGAG**TAACTA**CTGCCCCACTCC-3′.

Reporter assays

Effector plasmids expressing *Dlx2* under the control of a CMV promoter were constructed by insertion of a PCR amplified 1020 bp *Dlx2* cDNA (courtesy Dr John Rubenstein, University of California, San Francisco) into the pcDNA3 vector (Invitrogen). Reporter plasmids were constructed by inserting a 274 bp R1-pro fragment from position 57, 445, 126–57, 445, 399, chromosome 13, *TrkB* 5′ upstream region (Ensembl, ENSMUSG00000055254) into the pGL3 basic promoter vector (Promega, Madison, WI, USA).

Transient co-transfection experiments were performed in the HEK293 human embryonic kidney cell line (ATCC, Manassas, VA, USA). HEK293 cells were grown and maintained in alpha Dulbecco's modified Eagle's medium (αDMEM) supplemented with 7.5% fetal bovine serum, 2.5% calf serum and 1% penicillin–streptomycin at 37°C with 5% CO_2. Cells were seeded 24 h before transfection at a density of $1 \times 10^7/36$ mm^2 dish. Cells were transiently transfected using Lipofectamine 2000 reagent (Invitrogen). All transfections contained pRSV-β-gal (Promega) as a control for transfection efficiency. Luciferase activity was measured using the Luciferase Reporter Assay System (Promega) and a standard luminometer (Molecular Devices, Sunnyvale, CA, USA).

Retinal explants and retroviral transduction

Replication-incompetent ecotropic pMXIE retroviruses encoding murine *Dlx2* (pMXIE-EGFP/*dlx2*) or *Dlx1* (pMXIE-EGFP/*dlx1*) were obtained by inserting 999 bp *Dlx2* or 768 bp *Dlx1* cDNA (courtesy Dr John Rubenstein) into the pMXIE-EGFP retroviral vector (courtesy Dr D. Van der Kooy, University of Toronto, 26). Eyes were dissected from embryos in sterile 1× PBS and transferred to dishes containing DMEM/F12 media (Gibco/Invitrogen). Retinas were dissected under sterile

conditions from eyes with the lens and iris intact and transferred onto Millicell-CM 0.4 μM filters (Millipore) with the lens facing away from the membrane. Filters were transferred to 6-well culture plates containing media enriched with 1× N2 supplement, 1× MEM sodium pyruvate, 2 mM L-glutamine (all Gibco/Invitrogen), 5 μg/ml Insulin (Sigma), 1 U/ml penicillin/1 mg/ml streptomycin (Sigma), 1:10 dilution of retroviral solution (500 000 PFU/ml pMXIE-EGFP, 750 000 PFU/ml pMXIE-EGFP/*dlx1*, 750 000 PFU/ml pMXIE-EGFP/*dlx2*) and 0.1 mg/ml of polybrene (Sigma). Media was exchanged every 2 days. Retrovirus and polybrene were included only in the initial culture media. Explants were cultured at 37°C with 5% CO_2 in a humidified incubator for 10 days.

Primary retinal cell culture

E18.5 CD-1 mice retinas were dissociated and collected in Hank's Balanced Salt Solution (HBSS) and incubated for 10 min at room temperature with 0.05 mg/ml trypsin (Gibco). Soybean trypsin inhibitor (Sigma) was added to the final concentration of 2 mg/ml. The cells were then pelleted by centrifugation (1200 r.p.m., 5 min), resuspended and gently triturated to single-cell suspension in HBSS containing 100 μg/ml DNase I (Sigma). The cell suspension was transferred to a tube containing Neurobasal medium with B-27 supplement (Gibco) and 1× antimycotic antibiotic. Cells were counted and 3×10^5 cells were plated per well (poly-D-lysine- coated 12-well plate) and cultured at 37°C with 5% CO_2.

Transfection of primary retina cells with siRNA

Two duplex siRNAs were designed to target mouse *Dlx2* coding sequence and a control siRNA was synthesized to scrambled *Dlx2* coding sequence (Invitrogen) as follows: m*Dlx2*-R1-sense: 5′-(Fluo)GGAAGACCUUGAGCCUGAAdTdT, m*Dlx2*-R1-antisense: 5′-UUCAGGCUCAAGGUCUUCCdTdT; m*Dlx2*-R2-sense: 5′-(Fluo) UCUGGUUCCAGAACCGCCGdTdT-3′, m*Dlx2*-R2-antisense: 5′-CGGCGGUUCUGGAACCAGAdTdT-3′; control sense: 5′-(Fluo) UUCUCCGAACGUGUCACGUdTdT-3′, control antisense: 5′-ACGUGACACGUUCGGAGAAdTdT-3′. Transient transfection using Lipofectamine 2000 (Invitrogen) was carried out on the second day of tissue culture. siRNA to a final concentration of 40 nM (following Qiagen RNAifect transfection handbook protocol) was used. Cells were washed with cold PBS and lysed in RNA-bee (Tel-Test, Inc.); triplicate lysates were pooled and total RNA was purified according to the manufacturer's protocol 48 h after transfection.

Reverse transcription PCR

For reverse transcription (RT) PCR experiments, 1 μg of total RNA was used as a template to synthesize first-strand cDNA. Prior to the RT step, RNA samples were treated with DNase I (Sigma) for 15 min at room temperature to digest the genomic DNA; stop solution was added and samples were incubated at 70°C for 10 min to inactivate the DNase I, and then put immediately on ice. The total RT reaction volume was 20 μl and the

iScript^{TM} cDNA synthesis kit (Bio-Rad) was used with the following conditions: 5 min at 25°C, 30 min at 42°C and 5 min at 85°C. The cDNA served as a template for *Dlx2*, TrkB and GAPDH amplification. A 50 µl PCR reactions were performed, containing: 5 µl 10× PCR buffer, 3 µl MgCl₂ (25 mM), 1 µl dNTP (10 mM each), 1 µl each primer (10 µM), 2 µl cDNA, 10 µl 5× Qbuffer and 3 U HotStar Taq DNA Polymerase (Qiagen). PCR amplification conditions were: 94°C, 15 min for one cycle; 94 C, 30 s, 57°C, 30 s, and 72 C, 1 min for 39 cycles and an extension cycle at 72°C for 10 min. The PCR products were run on a 1.5% agarose gel with ethidium bromide. For RT-PCR, the oligonucleotide primers used were: *Dlx2*-F(p6): ccaaactcaggtcaaaatctg, *Dlx2*-R(p2): tta-gaaaatcgtcccgcg; mTrkB-F1: accttgacttgtctgacctgat, mTrkB-R1: cttctcctacaaggttttctgc; GAPDH-F: ctcatgac-cacagtccatgc, GAPDH-R: cacattggggggtaggaacac.

Cell counting and statistical analysis

For quantification of TrkB expression, paired *Dlx1/Dlx2* mutant and wild-type retinas were taken at regularly spaced intervals in order to completely survey each retina. Five sets of eyes consisting of one *Dlx1/Dlx2* homozygous mutant and one wild-type eye from littermate pairs were used for quantification at E13.5, E16.5 and E18.5. Eyes were sectioned at 12 µM. Sections through the widest region of the optic nerve head were used as a centered start point and were matched histologically. The start section and sections 120 and 240 µM above and below were used for immunostaining. For E13.5 and E16.5 sections 60 and 120 µM above and below the start section were used due to smaller eye size. Sections were fluorescently labeled for TrkB expression. Counts and statistical analysis was performed as previously described (17).

For retroviral transduction studies, pairs of sections from each explant were immunoassayed with cell-type specific markers. Sections were then imaged by confocal laser microscopy. Green fluorescent cells were counted to represent the total number of transduced cells. Cells with both green and red fluorescence were then counted to identify transduced cells expressing a particular marker. The proportion of transduced cells expressing a specific marker was then determined. Mean counts from paired tissues provided a representative proportion of labeled cells for the explants. The Student's *t*-test was utilized to make comparisons between proportions of marker expression among cells transduced by pMXIE empty vectors, pMXIE/*dlx1* vectors and pMXIE/*dlx2* vectors.

Microscopy and imaging

Fluorescent images were acquired using an Olympus IX81 inverted microscope equipped with a Fluoview FV500 confocal laser scanning system (Olympus Optical Co., Tokyo, Japan). An Olympus BX51 microscope equipped with a SPOT 1.3.0 digital camera (Diagnostic Instruments Inc., Sterling Heights, MI, USA) was used for non-fluorescent image capture. Images were processed using Adobe Photoshop 5.5 (Adobe Systems, Mountain View, CA, USA) and were formatted, resized and rotated for the purposes of presentation.

RESULTS

TrkB is expressed from E12.5 and is restricted to RGCs and amacrine cells in the murine retina

In order to define temporal and spatial localization of TrkB expression in the developing mouse retina, we used a well-characterized antibody to TrkB (27–30) for immuno-histochemistry. Onset of TrkB expression occurred at E12.5 (Figure 1A) with expression occurring in migrating cells in the central retinal neuroepithelium, the anatomic region from which the ganglion cell layer (GCL) originates. Some non-specific staining is evident adjacent to ventricles, along epithelial edges and in the peripheral region of the retina. This is an artefact of the immuno-histochemical staining procedure, when the antibody has minimal epitope to bind (data not shown). At E13.5 there is extensive expression of TrkB in the vitreal (inner) region of the central retina (Figure 1B). TrkB expression in the inner retina continues throughout embryonic development (Figure 1C and D) with expression restricted to the recently established GCL. By P14 lamination of the murine retina is established (Figure 1E). TrkB expression is found in the GCL (Figure 1E, arrows) without expression identified in the inner nuclear layer (INL) or outer nuclear layer (ONL). In the adult retina, expression of TrkB remains primarily restricted to the GCL (Figure 1F, arrows). However, expression of TrkB can now be identified in the INL (Figure 1F, asterisk) and in the corresponding inner plexiform layer (IPL). Expression of many amacrine cell subtype markers occurs very late in retinogenesis; a good example is tyrosine hydroxylase (16). The onset of Trkb expression in amacrine cells is after P14 (also refer to Supplementary Figure 3C).

Immunofluorescent co-localization studies with cell-type-specific antibodies to retinal ganglion, amacrine, horizontal, bipolar cells and cone and rod photoreceptors were performed to confirm the classes of cells expressing TrkB (Supplementary Figure 1–3). When evaluating these experiments, it is important to note that up to 50% of cells in the GCL are displaced amacrine cells in adult murine retinas (16). Co-expression with Brn3b and Islet1 transcription factors, markers expressed in RGCs (31–33) confirmed that TrkB expressing cells in the GCL were indeed RGCs (Supplementary Figures 1 and 2). Co-localization of TrkB with Islet1 and Brn3B was detected at E13.5 indicating that the onset of TrkB expression begins soon after establishment of RGC differentiation (Supplementary Figure 1C, *Islet1*; Supplementary Figure 2C, *Brn3B*). Co-localization with syntaxin, a marker of amacrine cells (34) was identified in the IPL and in a subpopulation of cells in the INL of the adult retina (Supplementary Figure 3C). Interestingly, there was no co-expression with choline acetyl-transferase (ChAT), a marker of cholinergic amacrine cells (35) (Supplementary Figure 3F) indicating that only a subset of amacrine cells express TrkB. Co-expression could not be detected with markers of horizontal (Prox1, 36)
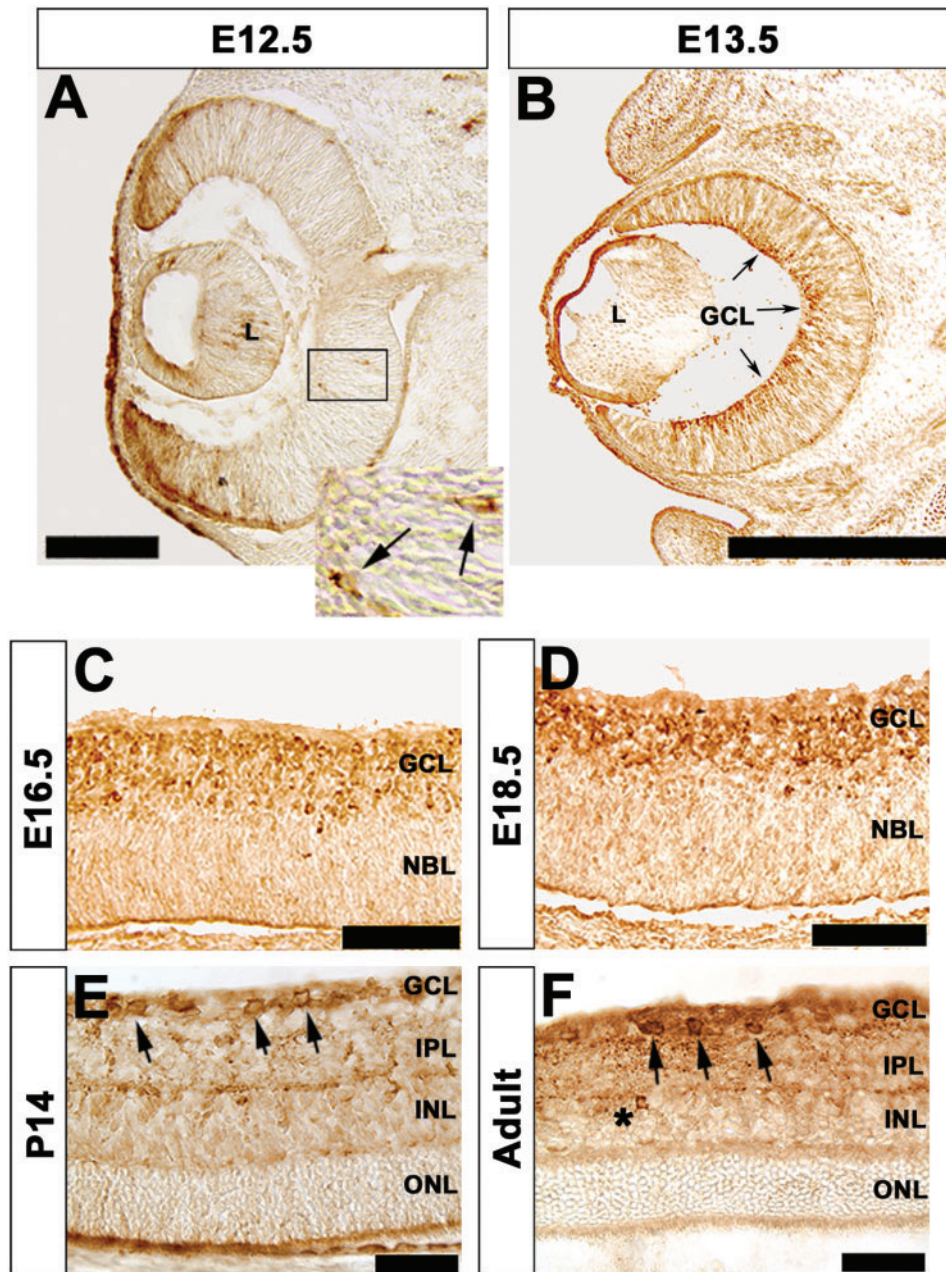
Figure 1. Characterization of TrkB protein expression in the developing murine retina. (**A**) Immunohistochemical localization of TrkB protein in E12.5 retina. Only a few cells express TrkB in the central inner retina; the GCL originates from this region (A, box; insert, arrows). Immunostaining of the retinal pigment epithelium along the ophthalmic ventricle and at other epithelial surfaces (presumptive cornea, within the lens ventricle) is non-specific. (**B–D**) Expression of TrkB becomes restricted to the inner retina from E13.5 to E18.5. By E16.5 TrkB expression is localized to a clearly defined GCL (C). (**E**) TrkB is localized to the GCL at P14 (E, arrows). (**F**) TrkB expression is ultimately restricted to RGCs in the adult retina (F, arrows) as well as in isolated amacrine cells (F, asterisk). Scale bars: (A) 125 μM; (B) 500 μM; (C, D) 100 μM; (E, F) 50 μM. Insert in (A) represents a 3.5-fold enlargement. GCL, ganglion cell layer; INL, inner nuclear layer; IPL, inner plexiform layer; L, lens; NBL, neuroblastic layer; ONL, outer nuclear layer.

or bipolar cells (Chx10, 37). There was no co-expression with markers of rod (Rho4D2, 38) or cone photoreceptors (PNA, 39) in the ONL or photoreceptor outer segments (Supplementary Figure 3I, L, O and R), although there was co-expression of PNA in the IPL, a region in the mouse retina known to express PNA but not cone photoreceptors (40). Hence, TrkB is expressed in the

RGC and amacrine cell populations of the adult retina localized to the GCL, IPL and INL.

DLX2-expressing cells co-express TrkB in the developing and adult murine retina

Previously, expression of DLX2 was demonstrated by E12.5 in the murine retina (15). In this study, DLX2

immunostaining was first detected in the dorsal retinal neuroepithelium by E11.5, where early RGC begin to differentiate (Figure 2B). DLX2-expressing cells are found in both dorsal and ventral retina by E12.5 (Figure 2E) with only rare TrkB co-expression (Figure 2F); however, those cells co-expressing TrkB can be readily identified by E13.5 (Figure 2I). In the E13.5 presumptive GCL, the proportion of cells expressing DLX2 is 41.5%, TrkB is 18.2% and those cells co-expressing DLX2 and TrkB is 8.7%. DLX2/TrkB double-positive cells are found in the inner retina at this stage with DLX2 single-positive cells located in the outer retina. These DLX2 single-positive cells primarily identify later born neurons migrating to the inner retina. By E16.5, the majority of DLX2 expressing neurons are located in the inner retina in the newly established GCL (Figure 2K). There is now extensive co-expression with TrkB among the DLX2 positive cells (Figure 2L). TrkB single-positive cells can be identified in the GCL (Figure 2L, arrows) at this stage as well as DLX2 single-positive cells migrating from the outer retina to the inner retina (Figure 2L, asterisk). By E18.5 DLX2/TrkB co-expressing cells are predominant throughout the GCL (Figure 2O). TrkB single-positive cells can still be identified but now constitute a minority of the TrkB population in the GCL (Figure 2O, arrows). DLX2 single-positive cells are also evident in the inner neuroblastic layer (NBL) as the INL begins to be established (Figure 2O, asterisks). In the adult retina, co-expression of DLX2 and TrkB is found amongst RGCs in the GCL as well as in the INL (Figure 2R, arrows, asterisk). TrkB single-positive neurons in the GCL and INL (Figure 2R, plus) are now rare. These results demonstrate that the onset of DLX2 expression precedes TrkB expression in the embryonic GCL by 1–2 days. The onset of TrkB expression amongst DLX2-expressing neurons appears upon their migration to the inner retina. This finding supports DLX2's potential role as a transcriptional regulator of TrkB expression in this RGC population.

DLX2 binds to a region of the TrkB proximal promoter *in vivo*

The mouse TrkB gene spans ~328 kb and contains 17 introns and 18 exons. In order to determine whether DLX2 directly binds to genomic DNA sequences within the *TrkB* gene locus we selected candidate-binding regions based upon groups of putative TAAT/ATTA homeodomain DNA binding motifs: one region (termed R1-pro) was located at nucleotides 57, 445, 126–57, 445, 399 (chromosomal numbering) (Figure 3A and B). R1-pro is located in the TrkB proximal promoter 842 bp 5′ of exon 1 and contains three TAAT/ATTA motifs; the latter two overlap. ChIP was performed on E16.5 retinal tissue and also E16.5 hindbrain tissue (which does not express Dlx genes) was used as a negative control. Oligonucleotide primers encompassing R1-pro were designed (Figure 3B, italics) and PCR analysis was performed. Mouse genomic DNA was utilized as a positive control for the PCR reaction. DLX2 bound to R1-pro in the E16.5 retina *in vivo* (Figure 3C). R1-pro could not be identified by ChIP in E16.5 hindbrain, nor could this region be
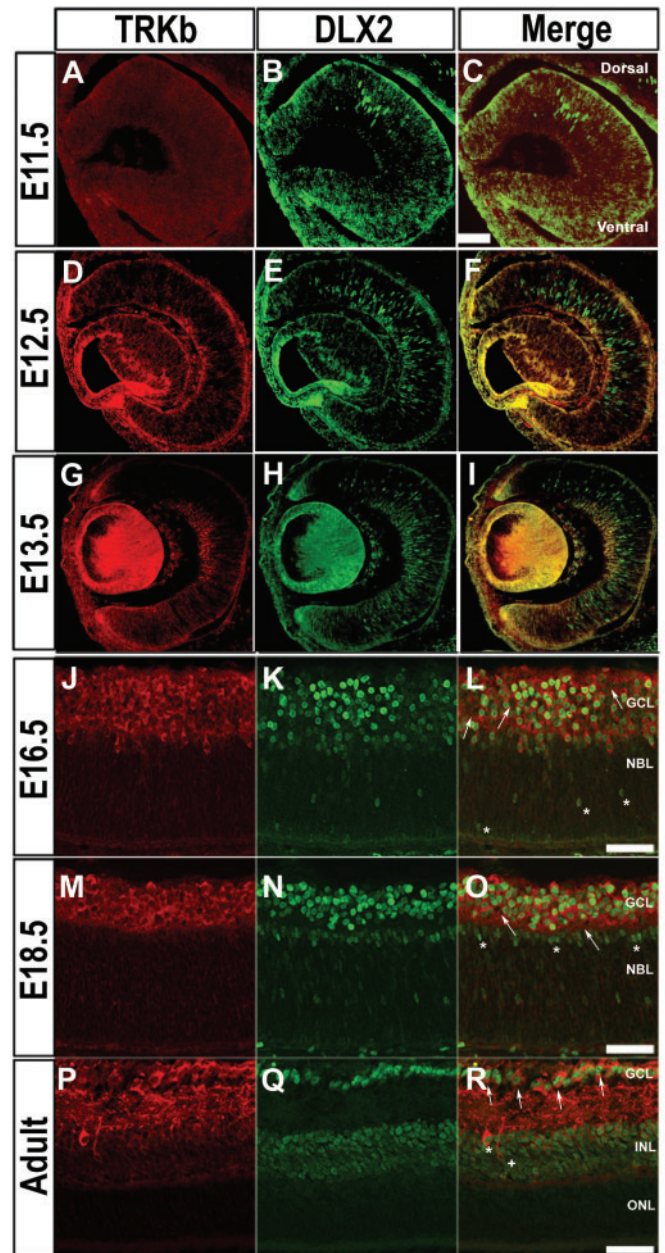
Figure 2. Co-localization of TrkB with DLX2 in the murine retina. (**A**–**C**) DLX2 is first expressed in the dorsal retinal neuroepithelium at E11.5 (B), whereas TrkB is not yet expressed in the retina at this embryonic stage (A). (**D**–**F**) At E12.5, there is onset of TrkB expression (D), but minimal co-expression with DLX2 whose domain of expression is extended to the ventral retina (F). (**G**–**I**) TrkB is co-expressed with DLX2 in cells of the central inner retina at E13.5. DLX2-positive TrkB-negative cells are located in the outer retina (I). (**J**–**L**) TrkB is co-expressed with DLX2 in cells of the inner retina within the GCL at E16.5 (L). TrkB and DLX2 single-positive cells may still be identified at this stage (L, arrows, asterisks). (**M**–**O**) TrkB is co-expressed with DLX2 in the GCL at E18.5 (O). Single-positive TrkB expressing cells within the GCL are present (O, arrows) as are DLX2 single positives within the inner NBL (O, asterisks). (**P**–**R**) TrkB is co-expressed with DLX2 in cells of GCL (R, arrows) and INL (R, asterisk) in the adult retina (R). A TrkB single-positive cell within the INL is evident within this photomicrograph (R, plus). Scale bars: (C) 100 μM; (L, O, R) 50 μM.

Figure 3. Genomic organization of the mouse *TrkB* gene, location of candidate homeoprotein binding sites, and confirmation that DLX2 binds to the TrkB pro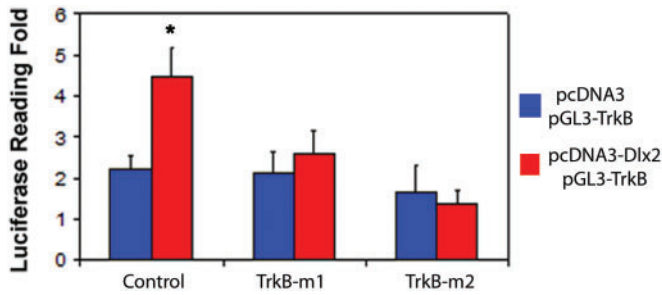ximal promoter in embryonic retina *in vivo*. (**A**) *TrkB* is located on murine chromosome 13 and contains 18 exons and 17 introns. Putative DLX2-binding regions are located within the 5′ proximal promoter region (R1-pro). (**B**) Sequence and organization of candidate homeodomain DNA-binding motifs in the *TrkB* gene. Candidate TAAT/ATTA homeodomain-binding motifs are underlined. PCR oligonucleotide primer sites are in italics and boxed. (**C**) E16.5 retina was cross-linked and immunoprecipitated with specific DLX2 antibodies following a modified chromatin immunoprecipitation (ChIP) protocol. After isolation of genomic DNA fragments bound to DLX2 homeoprotein, PCR using oligonucleotide primers to the proximal promoter (R1-pro) of the *TrkB* gene was performed. Total genomic DNA was used as a positive control. PCR products were subcloned and sequence-verified. E16.5 hindbrain was utilized as a tissue-negative control for ChIP assays.

identified after ChIP was performed without the DLX2 antibody (Figure 3C). Oligonucleotide primers were also generated to flank six other candidate homeodomain-binding regions within the TrkB proximal promoter other than R1-pro. DLX2 binding was not detected using these primers, demonstrating *in vivo* DLX2-binding specificity at R1-pro (Supplementary Figure 4).

EMSA was used to provide *in vitro* evidence of DLX2 binding specificity to R1-pro regulatory elements. Recombinant DLX2 protein binds to R1-pro resulting in characteristic gel shifts (Figure 4A, lane 2). Incubation with a specific DLX2 antibody resulted in a 'supershift' of bands for R1-pro (Figure 4A, lane 4). The presence of more than one band in the 'supershift' experiments may be the result of protein (recombinant or antibody) degradation and/or possible homodimerization of recombinant DLX2 proteins; this result is similar to those obtained using specific DLX antibodies and recombinant DLX proteins when characterizing regions of the *Dlx5/6* intergenic enhancer (25) or the Neuropilin-2 promoter (41) as candidate *Dlx* transcriptional targets. A control antibody did not produce a supershift for this region, although a non-specific band was seen (Figure 4A, lane 5). Hence, DLX2 specifically binds to the R1-pro region of the *TrkB* gene *in vitro*. Furthermore, incubation of E13.5 retina nuclear extracts

Figure 4. DLX2 binds to TrkB proximal promoter elements isolated by chromatin IP. (**A**) EMSA were performed using recombinant DLX2 protein and radiolabeled R1-pro oligonucleotide probes, with cold competition using unlabeled probe (A, lane 3) and specific DLX2 antibody 'supershift' assays (A, lane 4). Lane 1: labeled R1-pro alone. Lanes 2–5: labeled R1-pro probes were incubated with rDLX2 (2), rDLX2 and unlabeled R1-pro (3), rDLX2 and anti-DLX2 (4) and rDLX2 and a control antibody (5). (**B**) EMSA was also done using embryonic retinal nuclear extracts and radiolabeled R1-pro oligonucleotide probes containing either the first (TrkB motif 1, lanes 1–5) or second (TrkB motif 2, lanes 6–10) candidate homeodomain binding sites, with cold competition using unlabeled probe (B, lanes 3 and 8) and specific DLX2 antibody 'supershift' assays (B, lanes 5 and 10). Lanes 1, 6: labeled R1-pro alone. Lanes 2–10: labeled R1-pro probes were incubated with nuclear extract (2,7), nuclear extract and unlabeled TrkB motifs (3,8), nuclear extract and a control antibody (4,9) or nuclear extract and anti-DLX2 (5,10).

with radiolabeled oligonucleotide probes containing either candidate homeodomain-binding region (Figure 4, TrkB motif 1, B lanes 1–5; TrkB motif 2, B lanes 6–10) also demonstrated specific gel shifts, thereby confirming binding of endogenous DLX2 to the TrkB proximal promoter *in vitro* (Figure 4B, lanes 2 and 7); these gel shifts were not visualized when retinal nuclear extracts were incubated with unlabeled probes (Figure 4B, lanes 3 and 8) or labeled probes containing mutant homeodomain-binding motifs (Supplementary Figure 5, lanes 6 and 12). Similarly, incubation with a specific but not a control antibody resulted in supershifted bands (Figure 4B, lanes 5 and 10). Incubation of nuclear extracts obtained from embryonic liver, tissue that does not express DLX2, did not show specific gel shifts or supershifts (Supplementary Figure 5). These experiments support the specificity of DLX2 binding to regions of the TrkB proximal promoter identified by chromatin immunoprecipitation *in situ* and that either regulatory binding domain within the R1-pro region is required for binding to endogenous DLX2.

DLX2 activates TrkB promoter and enhancer elements *in vitro*

In order to demonstrate the functional significance of DLX2 binding to the TrkB proximal promoter, luciferase reporter gene assays were performed. *Dlx2* co-transfection

Figure 5. *Dlx2* transfection activates transcription of TrkB regulatory element luciferase reporter genes *in vitro*. In HEK 293 cells, luciferase gene reporter constructs containing either the wild-type proximal promoter region of TrkB isolated by chromatin immunoprecipitation (R1-pro) or mutant candidate homeodomain-binding sites (TrkB-m1 or TrkB-m2) were co-transfected with expression constructs for *Dlx2*. *Dlx2* co-transfection activated wild-type but not mutant R1-pro reporter gene expression. Error bars represent SEM; *denotes $P < 0.05$.

with the *TrkB* R1-pro vector resulted in increased luciferase expression (Figure 5). Observed normalized increases were ~2-fold for the R1-pro ($P < 0.05$). Using site-directed mutagenesis (25), mutation of either candidate TAAT/ATTA DNA-binding motif in the R1-pro region (Figure 3B) was accomplished. *Dlx2* co-transfection with these mutant *TrkB* R1-pro constructs (TrkB-m1, TrkB-m2) did not result in activation of reporter gene expression (Figure 5). These results support a functional role for DLX2 as a transcriptional activator of TrkB expression via binding at these regulatory sites.

Loss of function of Dlx1/Dlx2 results in decreased expression of TrkB in the developing murine retina

To determine whether loss of *Dlx* function affects TrkB expression *in vivo*, the *Dlx1/Dlx2* double mutant retina was studied. Mutant and wild-type retinas at E13.5, E16.5 and E18.5 were characterized with regards to TrkB protein expression. At E13.5, expression of TrkB was relatively unaffected in *Dlx1/Dlx2* mutant retinas compared with wild-type littermates (Figure 6B and E). Quantitative analysis identified a trend towards fewer TrkB expressing cells in the *Dlx1/Dlx2* mutants (Figure 6A), although the differences in TrkB+ cells did not reach statistical significance ($T = 2.78$, $P = 0.05$, $N = 5$). However, by E16.5, there were markedly fewer TrkB expressing cells in the mutant retinas (Figure 6C and F) with a significant 43% reduction ($T = 9.53$, $P < 0.05$, $N = 5$) (Figure 6A, *asterisk*). The reduction in TrkB-expressing cells was still evident at E18.5 (Figure 6D and G). At this stage there was a 30% reduction ($T = 10.43$, $P < 0.05$, $N = 5$) (Figure 6A, plus). Hence, TrkB expression is significantly reduced in the *Dlx1/Dlx2* double knockout retina at E16.5 and E18.5.

Gain of Dlx2 function in retinal explant cultures results in increased TrkB expression and increased expression of RGC and amacrine cell markers

Retroviral transduction of E18.5 retinal explant cultures with pMXIE-EGFP or pMXIE-EGFP/*dlx2* was
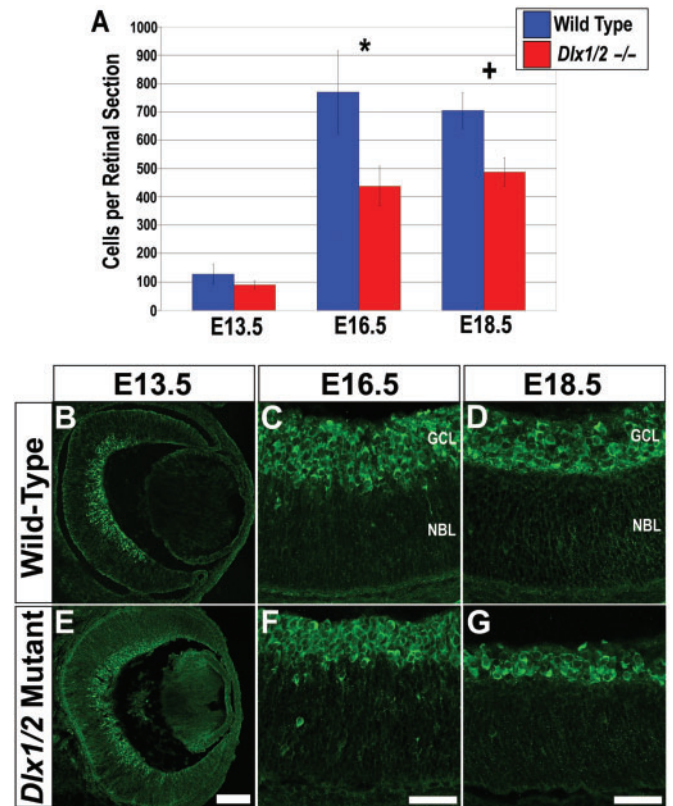
Figure 6. TrkB expression in the *Dlx1/Dlx2* mutant retina. (**A**) Quantification of TrkB expressing cells in the *Dlx1/Dlx2* mutant. At E13.5 there is no significant difference between the number of TrkB-expressing cells in the *Dlx1/Dlx2* mutant retina compared with wild-type controls ($T = 2.78$, $P = 0.05$, $N = 5$). At E16.5 (A, asterisk) and E18.5 (A, plus) there is a significant reduction in the number of TRKB-positive cells in the neural retina ($T = 9.53$, $P < 0.05$, $N = 5$ for a 43% reduction at E16.5; $T = 10.43$, $P < 0.05$, $N = 5$ for a 30% reduction at E18.5). (**B–G**) Expression of TrkB in the wild-type and *Dlx1/Dlx2* mutant murine retina. By E16.5 differences in the expression of TrkB are evident in *Dlx1/Dlx2* mutant (F) as compared to wild-type retinas (C) with fewer TrkB-expressing cells identifiable in the GCL. This difference is also observed at E18.5 (D, wild-type; G, mutant). Error bars represent SDs. Scale bars: (A) 100 μM; (F, G) 50 μM.

performed in order to determine whether gain of *Dlx2* function is sufficient to alter expression of TrkB or markers of specific retinal cell classes. Although efficiency of transduction is low (<5%) due to the poor penetration of exogenously applied retrovirus as well as the relatively small number of proliferating cells, one can readily identify and characterize the transduced cells that express GFP. Explants transduced with pMXIE-EGFP retrovirus co-localized with TrkB protein in 32% of transduced cells, as identified by GFP fluorescence and TrkB IF. There was a significant ($T = 5.67$, $P < 0.05$, $N = 5$) increase in co-localization with TrkB (to 62%) in cells transduced by pMXIE-EGFP/*dlx2* (Figure 7A, asterisk). Transduction with pMXIE-EGFP/*dlx2* as compared to pMXIE-EGFP also resulted in significant increases in co-localization with Islet1 (42 versus 23%, $T = 4.17$, $P < 0.05$, $N = 5$), a marker of RGCs and syntaxin (46 versus 29%, $T = 6.04$, $P < 0.05$, $N = 5$), a general marker for amacrine cells (Figure 7A, hash, plus). No significant differences were
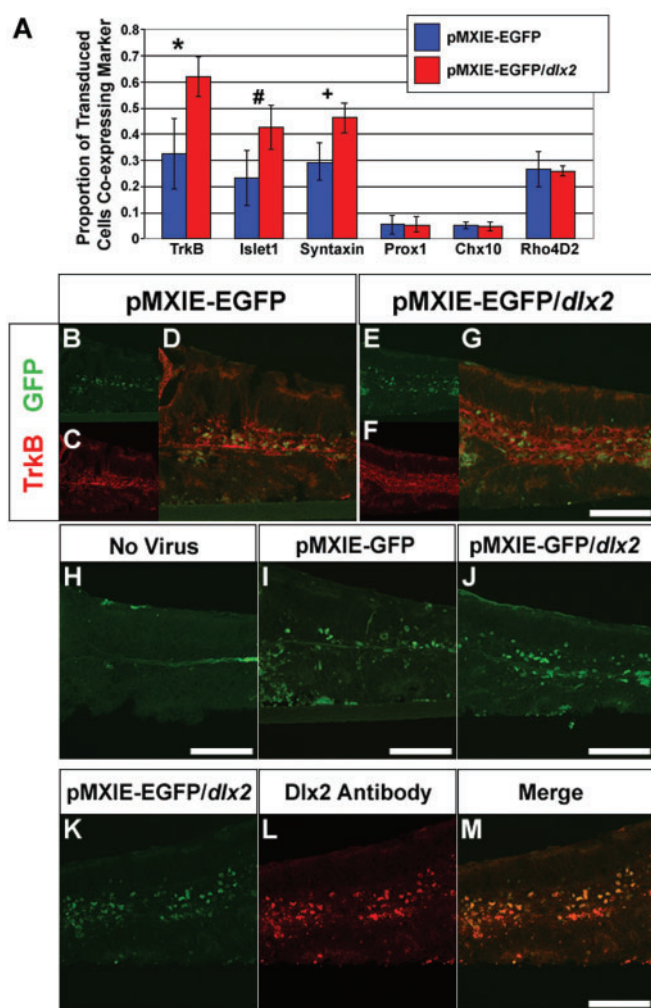
Figure 7. Retroviral transduction of Dlx2 in embryonic retinal explants. (**A**) Quantification of co-expression of EGFP and TrkB or markers for retinal cell class following transduction of retinal explants with either pMXIE-EGFP or pMXIE-EGFP/*dlx2* retrovirus. Markers for cell classes included: Islet1 for RGCs, syntaxin for amacrine cells, Prox1 for horizontal cells, Chx10 for bipolar interneurons and Rho4D2 for rod photoreceptors. Statistically significant differences could be identified between pMXIE-EGFP and pMXIE-EGFP/*dlx2*-transduced explants for TrkB (A, asterisk), Islet1 (A, hash) and syntaxin (A, plus). (**B–G**) Co-expression of EGFP and TrkB in pMXIE-EGFP or pMXIE-EGFP/*dlx2*-transduced explant cultures. (**H–J**) Expression of EGFP alone in control, pMXIE-EGFP, pMXIE-EGFP/*dlx2*-transduced explants. (**K–M**) Co-expression of EGFP and DLX2 in pMXIE-EGFP/*dlx2*-transduced explants. Error bars represent SDs. Scale bars: (G–J) 100 μM.

observed in co-expression of markers of horizontal cells, bipolar cells or rod photoreceptors (Figure 7A). Since some of the markers are expressed in more than one cell type, the percentages of cells transduced with pMXIE-EGFP/*dlx2* co-expressing lineage-specific markers may exceed 100%. Transduction of E18.5 retinal explant cultures with pMXIE-EGFP/*dlx1* retrovirus was also performed. No significant differences could be identified in co-localization with TrkB or of retinal cell-type markers in explants transduced by pMXIE-EGFP/*dlx1* compared to pMXIE-EGFP controls (Supplementary Figure 6 and
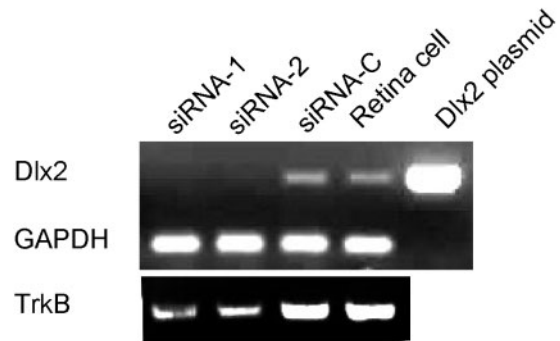
Figure 8. Knockdown of Dlx2 expression by siRNA in primary embryonic retinal cultures. Primary dissociated retinal cell cultures at E18.5 were transfected with duplex siRNAs targeting *Dlx2* coding sequences (siRNA-1 or siRNA-2) or a scrambled control siRNA (siRNA-C) and RNA was extracted at 48 h. A representative RT-PCR experiment (of three) is presented to compare levels of expression of *Dlx2* and TrkB among the experimental groups. Expression of GAPDH demonstrates equivalent loading of samples. Both siRNAs reduced *Dlx2* expression to almost undetectable levels and concomitantly decreased TrkB expression when compared to control siRNA and untransfected retinal cells. PCR of a *Dlx2* containing plasmid was performed as an additional control.

data not shown). These results support a specific function for DLX2 in the differentiation of RGCs and amacrine cells during retinogenesis, in part through the direct transcriptional activation of TrkB expression in the developing murine retina.

Knockdown of Dlx2 expression in primary embryonic retinal cultures results in decreased TrkB expression

Primary dissociated retinal cell cultures at E18.5 were transfected with duplex siRNAs targeting *Dlx2* coding sequences (siRNA-1 or siRNA-2) or a scrambled control siRNA (siRNA-C). Transfection with either siRNA resulted in almost undetectable *Dlx2* levels with a marked reduction of TrkB expression when compared to control siRNA transfected as well as untransfected retinal cells (Figure 8). Decreased TrkB expression in these *Dlx2* knockdown experiments in primary embryonic retinal cells corroborates the significant reduction of TrkB expression observed in *Dlx1/Dlx2* double knockout retina by E16.5 (Figure 6).

DISCUSSION

Post-natal TrkB expression becomes restricted to retinal ganglion and amacrine cells

TrkB expression in the developing retina has been characterized in the rat (42–44). Whereas TrkB expression in the murine retina has primarily focused on post-natal expression (5), we have demonstrated that TrkB expression in the murine retina begins at E12.5. Expression in central retinal neuroepithelial cells was coincidental with cells migrating from the proliferative region of the outer retina to the inner retina where differentiation occurs. In post-natal retina, expression of TrkB was restricted to the GCL and INL. Co-expression studies concluded that

TrkB expression was restricted to RGCs, from E13.5, and in amacrine cells, but only in the mature retina. While TrkB expression within adult murine RGCs has been well-documented (5,22), its expression in amacrine cells in the mouse has not been previously described, although this data supports earlier reports of TrkB expression in rat amacrine cells (42,43).

TrkB expression by E12.5 is significant as it demonstrates a much earlier onset of expression than previously reported. Initial RGC genesis begins at E10 with extensive RGC genesis occurring 2 days later (4,45). Our results suggest that TrkB expression occurs in these cells shortly after acquisition of RGC identity and TrkB may play a role in survival of RGCs during early retinogenesis. Nearly 50% of RGCs die during development (7) in two distinct phases (5). Previous studies have implicated TrkB in the regulation of the RGC death rate during the second post-natal phase when RGC projections form connections within the SC via target-derived BDNF signaling through TrkB in the early post-natal period (21). The first phase of RGC death occurs pre-natally with a peak at approximately E15 (6). This early phase of cell death may be mediated by signaling through the p75 receptor (6). Our results demonstrating early TrkB expression suggest that TrkB may also be involved in the regulation of RGC death during this first phase. The TrkB ligand BDNF is expressed in the murine retina as early as E10.5 (46) providing further evidence for TrkB signaling facilitating pre-natal RGC survival.

DLX2 directly binds and activates transcription of a TrkB regulatory element

In this study, we have demonstrated that the onset of DLX2 expression begins in the dorsal retina at E11.5, earlier than previously reported (15). DLX2 expression is maintained throughout retinogenesis with expression restricted to RGCs, amacrine cells and horizontal cells in the murine retina (15,16). We have demonstrated that DLX2 expression precedes the expression of TrkB by 1–2 days in the GCL and that DLX2-expressing neurons co-express TrkB in RGCs and amacrine cells. At E13.5, co-expression is limited to those DLX2-positive cells that have migrated to the nascent GCL. However, migrating DLX2+ neurons remain largely TrkB negative (Figure 2I). By E16.5 and E18.5 when migration is complete for most DLX2-positive cells, TrkB is co-expressed in nearly all observed DLX2+ cells in the GCL. The same pattern of DLX2 expression preceding TrkB expression was observed among amacrine cells in the GCL and INL. The spatio-temporal pattern of DLX2 and TrkB expression suggests the possibility that DLX2 may play a role in the transcriptional regulation of TrkB.

Little is known about the transcriptional regulation of TrkB. Thyroid hormone down-regulates TrkB expression in the rat brain through a novel response element (47). Retinoic acid treatment of SH-SY5Y human neuroblastoma cells induces a neuronal differentiation process featuring increased TrkB expression (48). Recent studies have demonstrated that the bHLH proteins E47 and NeuroD directly bind to E-boxes within the proximal

TrkB promoter activating TrkB expression in SH-SY5Y cells (49). Moreover, the Wilm's tumor transcription factor Wt1 activates TrkB by binding a Wt1 consensus motif in the human NTRK2 promoter. This regulation is necessary for the expression of TrkB in the epicardium and intramyocardial blood vessels (50). Herein, utilizing chromatin immunoprecipitation of embryonic retinal tissues, we have demonstrated that DLX2 directly binds to specific homeodomain-binding motifs within the *TrkB* promoter (termed R1-pro) *in vivo*. Specificity of DLX2 protein–TrkB promoter DNA interactions was confirmed by EMSA *in vitro* using recombinant DLX2 and nuclear extracts expressing endogenous DLX2 obtained from embryonic retina. Mutation of either candidate homeodomain DNA-binding region resulted in loss of specific gel shifts. Reporter gene assays demonstrated that DLX2 binding to R1-pro was functionally significant as there was transcriptional activation of this response elements and this activation was abrogated by mutating either TAAT/ATTA DNA-binding motif *in vitro*.

The temporal relationship of DLX2 and TrkB expression in subpopulations of RGCs, identification of DLX2 protein–TrkB DNA sequence complexes in embryonic retina *in vivo*, together with the transcriptional activation of these *TrkB* gene regulatory elements *in vitro* suggest that DLX2 may act to regulate *TrkB* gene expression in these RGCs to maintain their survival. These results demonstrate for the first time the regulation of TrkB gene expression by a homeodomain transcription factor. This study establishes a direct transcriptional relationship between a homeodomain protein involved in the differentiation of RGCs (17) and a neurotrophin receptor implicated in RGC survival (22).

Loss or gain of DLX2 function alters expression of TrkB in the developing retina

Dlx1/Dlx2 double mutant mice have increased embryonic retinal apoptosis resulting in a specific loss of approximately one-third of RGCs by E18.5 (17). We have demonstrated decreased TrkB expression in the *Dlx1/Dlx2* double knockout mouse. Importantly, a significant reduction of TrkB-expressing cells can be identified by E16.5 with this loss detected as early as E13.5. Thus, loss of TrkB expression precedes reduction of RGC numbers between E16.5 and E18.5 in the *Dlx1/Dlx2* double mutant. Establishing this time-line is important; a decreased RGC population would affect TrkB quantification, since TrkB is primarily expressed in this retinal cell subclass. Reduced TrkB expression prior to detection of RGC loss in the *Dlx1/Dlx2* mutant retina suggests a mechanism that may contribute to the increased RGC apoptosis. Moreover, acute knockdown of *Dlx2* expression in wild-type primary dissociated embryonic retinal cultures, also results in decreased TrkB expression. Rodent RGCs appear to be very sensitive to RNAi, with adult RGC in culture also showing efficient knockdown (51). These *Dlx2* knockdown experiments support our observations of significant reduction of retinal TrkB expression with the loss of both *Dlx1* and *Dlx2* function. Other transcription factors besides *Dlx1/Dlx2* are likely required for the expression of

TrkB, since a large proportion of TrkB-expressing cells remain in the *Dlx1/Dlx2* mutant retina. These unidentified genes are probably genetically upstream of *Dlx1/Dlx2* or in parallel pathways. Recently, the basic HLH gene *Mash1* has been shown to bind to a region of the *Dlx1/Dlx2* intergenic enhancer, using ChIP assays of developing forebrain (52). However, regulation of *Dlx* expression by Mash1 in embryonic retina has not yet been addressed.

We have shown that ectopic *Dlx2* expression driven by retroviral transduction of retinal explant cultures is sufficient for increased TrkB expression. Forced *Dlx2* expression also leads to increased expression of RGC and amacrine cell markers, although ectopic *Dlx2* expression may have occurred in both RGC as well as non-RGC progenitor populations. Hence, DLX2 promotes the differentiation of retinal progenitor cells toward an RGC or amacrine cell fate. Although TrkB is expressed in both RGCs and amacrine cells, it remains unclear whether RGC survival is facilitated by the TrkB signaling pathway. In support of this hypothesis, NeuroD, shown to directly activate TrkB expression (49) is sufficient to drive amacrine cell genesis, although it is not required for amacrine cell development (53).

Somewhat unexpected was our observation that forced expression of *Dlx1* by retroviral transduction did not alter expression of TrkB or any retinal cell class marker. The *Dlx1/Dlx2* double mutant demonstrates the requirement for both *Dlx1* and *Dlx2* function for correct CNS development (13,54). In the retina, *Dlx1* is expressed by E12.5 but its expression is downregulated at or just prior to birth, dependent on the mouse strain (16,17). DLX2, but not DLX1, binds to the *Dlx5/Dlx6* intergenic enhancer in neonatal forebrain and retina *in vivo* and only *Dlx2* activates expression of this enhancer element *in vitro* (25). We have primarily addressed *Dlx2* function in this manuscript due to the availability of specific polyclonal antibodies to study DLX2 expression and perform immunoprecipitation and 'supershift' gel shift assays. Of interest, DLX2 may be a more 'active' transcriptional activator (25) or repressor (41) than DLX1. In co-transfection experiments, *Dlx1* and *Dlx2* are not synergistic (25,41). Although our results support a limited requirement for *Dlx1* in retinal neurogenesis, loss of *Dlx1* function may also have a contribution to the retinal phenotype of the *Dlx1/Dlx2* double knockouts.

TrkB signaling has been demonstrated to inhibit the death of immature RGCs (21,22). Mice with null mutations of *TrkB* (22) have increased rates of RGC death during development. Similar increased developmental cell death within the *Dlx1/Dlx2* double mutant retina is also observed (17). Interestingly, loss of function of TrkB or BDNF does not affect the final number of RGCs (5,22,55). Therefore, independent mechanisms are proposed for the regulation of final RGC numbers. Within the *Dlx1/Dlx2* double mutant mouse there is a marked loss of cells expressing RGC markers. *Dlx1/Dlx2* knockout mice die shortly after birth (23). Consequently, the RGC phenotype of the mature retina of these mutants remains unknown. Studies of forebrain neurogenesis in *Dlx1/Dlx2* double mutants have demonstrated defects in interneuron differentiation and migration (13,41,54,56).

Hence, loss of *Dlx* function likely results in a more severe retinal phenotype than that displayed by TrkB mutation alone. The identification of other *Dlx* transcriptional targets in the retina may provide further insights into the role of *Dlx* genes during retinal cell differentiation and survival.

SUPPLEMENTARY DATA

Supplementary Data are available at NAR Online.

REFERENCES

1. Masland,R.H. (2001) The fundamental plan of the retina. *Nat. Neurosci.*, **4**, 877–886.
2. LaVail,M.M., Rapaport,D.H. and Rakic,P. (1991) Cytogenesis in the monkey retina. *J. Comp. Anat.*, **309**, 86–114.
3. Steimke,M.M. and Hollyfield,J.G. (1995) Cell birthdays in *Xenopus laevis* retina. *Differentiation*, **58**, 189–193.
4. Cepko,C.L., Austin,C.P., Yang,X., Alexiades,M. and Ezzidine,D. (1996) Cell fate determination in the vertebrate retina. *Proc. Natl Acad. Sci. USA*, **93**, 589–595.
5. Rohrer,B., LaVail,M.M., Jones,K.R. and Reichardt,L.F. (2001) Neurotrophin receptor TrkB activation is not required for postnatal survival of retinal ganglion cells in vivo. *Exp. Neurol.*, **172**, 81–91.
6. Frade,J.M. and Barde,Y.A. (1999) Genetic evidence for cell death mediated by nerve growth factor and the neurotrophin receptor p75 in the developing mouse retina and spinal cord. *Development*, **126**, 683–690.
7. Young,R.W. (1984) Cell differentiation in the retina of the mouse. *J. Comp. Neurol.*, **229**, 362–373.
8. Panganiban,G. and Rubenstein,J.L. (2002) Developmental functions of the Distal-less/Dlx homeobox genes. *Development*, **129**, 4371–4386.
9. McGuinness,T., Porteus,M.H., Smiga,S., Bulfone,A., Kingsley,C., Qiu,M., Liu,J.K., Long,J.E., Xu,D. *et al.* (1996) Sequence, organization, and transcription of the Dlx-1 and Dlx-2 locus. *Genomics*, **35**, 473–485.
10. Sumiyama,K., Irvine,S.Q., Stock,D.W., Weiss,K.M., Kawasaki,K., Shimizu,N., Shashikant,C.S., Miller,W. and Ruddle,F.H. (2002) Genomic structure and functional control of the Dlx3-7 bigene cluster. *Proc. Natl Acad. Sci. USA*, **99**, 780–785.
11. Ghanem,N., Jarinova,O., Amores,A., Long,Q., Hatch,G., Park,B.K., Rubenstein,J.L. and Ekker,M. (2003) Regulatory roles

of conserved intergenic domains in vertebrate Dlx bigene clusters. *Genome Res.*, **13**, 533–543.

12. Bulfone,A., Kim,H.J., Puelles,L., Porteus,M.H., Grippo,J.F. and Rubenstein,J.L.R. (1993) The mouse Dlx-2 (Tes-1) gene is expressed in spatially restricted domains of the forebrain, face, and limbs in midgestation mouse embryos. *Mech. Dev.*, **40**, 129–140.

13. Anderson,S.A., Qiu,M., Bulfone,A., Eisenstat,D.D., Meneses,J., Pederson,R. and Rubenstein,J.L.R. (1997a) Mutations of the homeobox genes Dlx-1 and Dlx-2 disrupt the striatal subventricular zone and differentiation of late born striatal neurons. *Neuron*, **19**, 27–37.

14. Liu,J.K., Ghattas,I., Liu,S., Chen,S. and Rubenstein,J.L.R. (1997) *Dlx* genes encode DNA-binding proteins that are expressed in an overlapping and sequential pattern during basal ganglia differentiation. *Dev. Dyn.*, **210**, 498–512.

15. Eisenstat,D.D., Liu,J.K., Mione,M., Zhong,W., Yu,G., Anderson,S.A., Ghattas,I., Puelles,L. and Rubenstein,J.L.R. (1999) DLX-1, DLX-2, and DLX-5 expression define distinct stages of basal forebrain differentiation. *J. Comp. Neurol.*, **414**, 217–237.

16. de Melo,J., Qiu,X., Du,G., Cristante,L. and Eisenstat,D.D. (2003) Dlx1, Dlx2, Pax6, Brn3b, and Chx10 homeobox gene expression defines the retinal ganglion and inner nuclear layers of the developing and adult mouse retina. *J. Comp. Neurol.*, **461**, 187–204.

17. de Melo,J., Du,G., Fonseca,M., Gillespie,L.A., Turk,W.J., Rubenstein,J.L.R. and Eisenstat,D.D. (2005) Dlx1 and Dlx2 function is necessary for terminal differentiation and survival of late-born retinal ganglion cells in the developing mouse retina. *Development*, **132**, 311–322.

18. Huang,E.J. and Reichardt,L.F. (2001) Neurotrophins: roles in neuronal development and function. *Ann. Rev. Neurosci.*, **24**, 677–736.

19. Sofroniew,M.V., Howe,C.L. and Mobley,W.C. (2001) Nerve growth factor signalling, neuroprotection, and neural repair. *Annu. Rev. Neurosci.*, **24**, 1217–1281.

20. Kalb,R. (2005) The protean actions of neurotrophins and their receptors on the life and death of neurons. *Trends Neurosci.*, **28**, 5–11.

21. Ma,Y.T., Hsieh,T., Forbes,M.E., Johnson,J.E. and Frost,D.O. (1998) BDNF injected into the superior colliculus reduces developmental retinal ganglion cell death. *J. Neurosci.*, **18**, 2097–2107.

22. Pollock,G.S., Robichon,R., Boyd,K.A., Kerkel,K.A., Kramer,M., Lyles,J., Ambalavanar,R., Khan,A., Kaplan,D.R. *et al.* (2003) TrkB receptor signalling regulates developmental death dynamics, but not final number, of retinal ganglion cells. *J. Neurosci.*, **23**, 10137–10145.

23. Qiu,M., Bulfone,A., Ghattas,I., Meneses,J.J., Christensen,L., Sharpe,P.T., Presley,R., Pedersen,R.A. and Rubenstein,J.L.R. (1997) Role of the Dlx homeobox genes in proximodistal patterning of the branchial arches: Mutations of Dlx1, Dlx2, and Dlx1 and Dlx2 alter morphogenesis of proximal skeletal and soft tissue structures derived from the first and second arches. *Dev. Biol.*, **185**, 165–184.

24. Qiu,M., Bulfone,A., Martinez,S., Meneses,J.J., Shimamura,K., Pederson,R.A. and Rubenstein,J.L.R. (1995) Null mutation of Dlx-2 results in abnormal morphogenesis of proximal first and second branchial arch derivatives and abnormal differentiation in the forebrain. *Genes Dev.*, **9**, 2523–2538.

25. Zhou,Q.P., Le,T.N., Qiu,X., Spencer,V., de Melo,J., Du,G., Plews,M., Fonseca,M., Sun,J.M. *et al.* (2004) Identification of a direct Dlx homeodomain target in the developing mouse forebrain and retina by optimization of chromatin immunoprecipitation. *Nucleic Acids Res.*, **32**, 884–892.

26. Hitoshi,S., Alexson,T., Tropepe,V., Donoviel,D., Elia,A.J., Nye,J.S., Conlon,R.A., Mak,T.W., Bernstein,A. *et al.* (2002) Notch pathway molecules are essential for the maintenance, but not the generation, of mammalian neural stem cells. *Genes Dev.*, **16**, 846–858.

27. Wang,S., Bray,P., McCaffrey,T., March,K., Hempstead,B.L. and Kraemer,R. (2000) p75(NTR) mediates neurotrophin-induced apoptosis of vascular smooth muscle cells. *Am. J. Pathol.*, **157**, 1247–1258.

28. Sakuma,K., Watanabe,K., Sano,M., Uramoto,I., Nakano,H., Li,Y.J., Kaneda,S., Sorimachi,Y., Yoshimoto,K. *et al.* (2001) A possible role for BDNF, NT-4 and TrkB in the spinal cord and muscle of rat subjected to mechanical overload, bupivacaine injection and axotomy. *Brain Res.*, **907**, 1–19.

29. Hardingham,G.E., Fukunaga,Y. and Bading,H. (2002) Extrasynaptic NMDARs oppose synaptic NMDARs by triggering CREB shut-off and cell death pathways. *Nat. Neurosci.*, **5**, 405–414.

30. Douma,S., Van Laar,T., Zevenhoven,J., Meuwissen,R., Van Garderen,E. and Peeper,D.S. (2004) Suppression of anoikis and induction of metastasis by the neurotrophic receptor TrkB. *Nature*, **430**, 1034–1039.

31. Liu,W., Khare,S.L., Liang,X., Peters,M.A., Liu,X., Cepko,C. and Xiang,M. (2000) All Brn3 genes can promote retinal ganglion cell differentiation in the chick. *Development*, **127**, 3237–3247.

32. Ma,W., Yan,R.T., Xie,W. and Wang,S.Z. (2004) bHLH genes cath5 and cNSCL1 promote bFGF-stimulated RPE cells to transdifferentiate toward retinal ganglion cells. *Dev. Biol.*, **265**, 320–328.

33. Mu,X. and Klein,W.H. (2004) A gene regulatory hierarchy for retinal ganglion cell specification and differentiation. *Semin. Cell. Dev. Biol.*, **15**, 115–123.

34. Barnstable,C.J., Hofstein,R. and Akagawa,K. (1985) A marker of amacrine cell development in rat retina. *Brain Res.*, **352**, 286–290.

35. Haverkamp,S. and Wässle,H. (2000) Immunocytochemical analysis of the mouse retina. *J. Comp. Neurol.*, **424**, 1–23.

36. Dyer,M.A., Livesey,F.J., Cepko,C.L. and Oliver,G. (2003) Prox1 function controls progenitor cell proliferation and horizontal cell genesis in the mammalian retina. *Nat. Genet.*, **34**, 53–58.

37. Chow,R.L., Snow,B., Novak,J., Looser,J., Freund,C., Vidgen,D., Ploder,L. and McInnes,R.R. (2001) Vsx1, a rapidly evolving paired-like homeobox gene expressed in cone bipolar cells. *Mech. Dev.*, **109**, 315–322.

38. Davidson,F.F., Loewen,P.C. and Khorana,H.G. (1994) Structure and function in rhodopsin: replacement by alanine of cysteine residues 110 and 187, components of a conserved disulfide bond in rhodopsin, affects the light-activated metarhodopsin II state. *Proc. Natl Acad. Sci. USA*, **91**, 4029–4033.

39. Chen,J., Tucker,C.L., Woodford,B., Szel,A., Lem,J., Gianella-Borradori,A., Simon,M.I. and Bogenmann,E. (1994) The human blue opsin promoter directs transgene expression in short-wave cones and bipolar cells in the retina. *Proc. Natl Acad. Sci USA*, **91**, 2611–2615.

40. Blanks,J.C. and Johnson,L.V. (1983) Selective lectin binding of the developing mouse retina. *J. Comp. Neurol.*, **221**, 31–41.

41. Le,T.N., Du,G., Fonseca,M., Zhou,Q.P., Wigle,J.T. and Eisenstat,D.D. (2007) Dlx homeobox genes promote cortical interneuron migration from the basal forebrain by direct repression of the semaphorin receptor neuropilin-2. *J. Biol. Chem.*, **282**, 19071–19081.

42. Jelsma,T.N., Friedman,H.H., Berkelaar,M., Bray,G.M. and Aguayo,A.J. (1993) Different forms of the neurotrophin receptor TrkB mRNA predominate in rat retina and optic nerve. *J. Neurobiol.*, **24**, 1207–1214.

43. Koide,T., Takahashi,J.B., Hoshimaru,M., Kojima,M., Otsuka,T., Asahi,M. and Kikuchi,H. (1995) Localization of TrkB and low-affinity nerve growth factor receptor mRNA in the developing rat retina. *Neurosci. Lett.*, **185**, 183–186.

44. Rickman,D.W. and Brecha,N. (1995) Expression of the proto-oncogene, Trk, receptors in the developing rat retina. *Vis. Neurosci.*, **12**, 215–222.

45. Young,R.W. (1985) Cell death during differentiation of the retina in the mouse. *Anat. Rec.*, **212**, 199–205.

46. Bennett,J.L., Zeiler,S.R. and Jones,K.R. (1999) Patterned expression of BDNF and NT-3 in the retina and anterior segment of the developing mammalian eye. *Invest. Ophthalmol. Vis. Sci.*, **40**, 2996–3005.

47. Pombo,P.M., Barettino,D., Espliguero,G., Metsis,M., Iglesias,T. and Rodriguez-Pena,A. (2000) Transcriptional repression of neurotrophin receptor trkB by thyroid hormone in the developing rat brain. *J. Biol. Chem.*, **275**, 37510–37517.

48. Encinas,M., Iglesias,M., Liu,Y., Wang,H., Muhaisen,A., Cena,V., Gallego,C. and Comella,J.X. (2000) Sequential treatment of SH-SY5Y cells with retinoic acid and brain-derived neurotrophic

factor gives rise to fully differentiated, neurotrophic factor-dependent, human neuron-like cells. *J. Neurochem.*, **75**, 991–1003.

49. Liu,Y., Encinas,M., Comella,J.X., Aldea,M. and Gallego,C. (2004) Basic helix-loop-helix proteins bind to TrkB and p21Cip1 promoters linking differentiation and cell cycle arrest in neuroblastoma cells. *Mol. Cell. Biol.*, **24**, 2662–2672.

50. Wagner,N., Wagner,C.D., Theres,H., Englert,C., Schedl,A. and Scholz,H. (2005) Coronary vessel development requires activation of the TrkB neurotrophin receptor by the Wilms' tumor transcription factor Wt1. *Genes Dev.*, **19**, 2631–2642.

51. Ahmed,Z., Suggate,E.L., Brown,E.R., Dent,R.G., Armstrong,S.J., Barrett,L.B., Berry,M. and Logan,A. (2006) Schwann cell-derived factor-induced modulation of the NgR/p75NTR/EGFR axis disin-hibitis axon growth through CNS myelin in vivo and in vitro. *Brain*, **129**, 1517–1533.

52. Poitras,L., Ghanem,N., Hatch,G. and Ekker,M. (2007) The proneural determinant MASH1 regulates forebrain Dlx1/2

expression through the I12b intergenic enhancer. *Development*, **134**, 1755–1765.

53. Morrow,E.M., Furukawa,T., Lee,J.E. and Cepko,C.L. (1999) NeuroD regulates multiple functions in the developing neural retina in rodent. *Development*, **126**, 23–36.

54. Anderson,S.A., Eisenstat,D.D., Shi,L. and Rubenstein,J.L.R. (1997b) Interneuron migration from basal forebrain to neocortex: dependence on Dlx genes. *Science*, **278**, 474–476.

55. Cellerino,A., Carroll,P., Thoenen,H. and Barde,Y. (1997) Reduced size of retinal ganglion cell axons and hypomyelination in mice lacking brain-derived neurotrophic factor. *Mol. Cell. Neurosci.*, **9**, 397–408.

56. Bulfone,A., Wang,F., Hevner,R., Anderson,S., Cutforth,T., Chen,S., Meneses,J., Pederson,R., Axel,R. *et al.* (1998) An olfactory sensory map develops in the absence of normal projection neurons or GABAergic interneurons. *Neuron*, **21**, 1273–1282.